

SEPARATION OF HEMICELLULOSES FROM *EUCALYPTUS* SPECIES: INVESTIGATING THE RESIDUE AFTER ALKALINE TREATMENT

WANXI PENG,^{*,**} LANSHENG WANG,^{*} MAKOTO OHKOSHI^{**} and MINGLONG ZHANG^{*}

^{*}*School of Materials Science and Engineering, Central South University of Forestry and Technology, Changsha 410004, China*

^{**}*Laboratory of Biomaterials Science, Kyoto Prefectural University, Kyoto, Japan*

✉ *Corresponding authors: Wanxi Peng, pengwanxi@163.com, and Makoto Ohkoshi, mohkoshi@kpu.ac.jp*

Received October 28, 2013

Hemicellulose, the second most abundant polysaccharide in nature, is an ideal biomass for bioconversion. However, it binds with cellulose and lignin to form the cell wall and efficient separation of *Eucalyptus* wood biomass components remains difficult. Therefore, the residue after alkaline treatment of *Eucalyptus* species was investigated and analyzed by FTIR, XRD, UV and SEM. The results showed that the crystallinity index of *Eucalyptus urophydis*, *Eucalyptus urophytis* and *Eucalyptus camaldulensis* lignocelluloses reached respective maxima of 63.49% (6 h), 58.29% (3 h), and 60.70% (9 h) in KOH solution. However, the lignin content in these residues was reduced by 10.1%, 8.38%, and 5.7%, respectively. After the alkaline treatment, most of the acetyl groups in the residue were broken down because the alkali treatment under the conditions used mostly cleaved the ester bonds. It was found that the hemicelluloses were dissolved after 3 h, while after 20 h, the pit membrane was dissolved, pits were penetrated, holes appeared in the cell wall, and cell gaps opened.

Keywords: *Eucalyptus urophydis*, *Eucalyptus urophytis*, *Eucalyptus camaldulensis*, hemicelluloses, separation characteristics

INTRODUCTION

Lignocellulosic biomass, which is the most abundant, renewable and inexpensive bioresource in the biosphere, accounts for approximately 50% of all biomass, and can be used to produce ethanol, food additives, organic acids, and other value-added bio-products.¹ Lignocelluloses mainly include cellulose, hemicellulose and lignin, and the components are closely associated with each other to comprise the cellular complex.¹ Feedstocks based on the separation of single fractions (extractives, cellulose, hemicelluloses, lignin) are each prepared by different means.² In recent years, bioconversion of hemicellulose has received particular attention due to its practical applications in various agro-industrial processes, such as efficient conversion of hemicellulosic biomass to fuels and chemicals, delignification of paper pulp, enhancement of animal feedstock digestibility, clarification of juices, and improvement in the consistency of beer.²⁻⁶ Pretreatment of hemicellulose is necessary and widely studied for bioconversion.

Hemicelluloses, which include xyloglucans,

xylans, mannans and glucomannans, and β -(1 \rightarrow 3,1 \rightarrow 4)-glucans, account for 25-50% of the cell wall in wood, and are the second-most abundant polysaccharides in plants.⁷ Compared with cellulose and lignin, hemicelluloses are the least stable of the active ingredients. It is highly desirable to separate hemicellulose efficiently from the cell wall, but it is typically destroyed during processing and use. Furthermore, efficient use of hemicellulose was not considered seriously because its separation from processing waste is difficult, and its potential use as a resource was unclear. With the development of biomass energy, wood hemicellulose was recognized for the preparation of biofuel sources.⁸ Various methods to obtain the maximum yield and purity of hemicellulose have been explored, including physical, thermal, chemical, biological approaches or their combinations.^{9,10} Wu *et al.* attempted to enhance hemicellulose recovery by steam explosion,¹¹ but the separation was ineffective. Brodeur *et al.* found that a pretreatment process could enhance hemicellulose

yields.¹² Hemicellulose can be obtained by alkali extraction and ethanol separation.¹³ Song *et al.* studied the extraction of hemicelluloses with pressurized hot water.^{14,15} Under the process conditions used, hemicelluloses may be degraded to weak acids, furan derivatives and phenolics that inhibit subsequent fermentation processes, leading to lower yields and productivities of the desired product⁸. Hemicelluloses were also obtained through biotechnology.¹⁶ In general, hemicellulosic preparations consist of several hemicellulosic molecules, which vary in structural characteristics. In view of this, several fractionation techniques, such as graded ethanol precipitation,¹⁷ ammonium sulfate precipitation, and anion-exchange chromatography,^{18,19} have been used to obtain more homogeneous fractions and thus explore structure-property relationships for these polymers.

The fractionation of hemicelluloses is a critical prerequisite for applications, in particular on a large industrial scale. The sub-fractionation of hemicelluloses may produce low-branched xylans and further yield xylose, an intermediate used in the production of xylitol, and a variety of xylo-oligosaccharides. Xylitol has already been used in food applications, such as chewing gum and toothpaste,²⁰ and could provide an alternative sweetener for diabetics.²¹⁻²⁴ Thus, the separation methods for hemicellulose will depend on the type of raw material used, the objective of the process and the desired product, all of which will directly affect the cost-benefit. However, hemicellulose binds with cellulose and lignin to form the cell wall and the individual and efficient separation of *Eucalyptus* wood biomass remains very difficult. Therefore, the separation characteristics of *Eucalyptus* hemicelluloses were investigated and analyzed by Fourier transform infrared (FTIR) spectroscopy, X-ray diffraction (XRD), ultraviolet light (UV) absorption and scanning electron microscope (SEM).

EXPERIMENTAL

Materials and reagents

Five-year-old *Eucalyptus urophylla* (*Eucalyptus urophylla* × *Eucalyptus tereticornis*) and *Eucalyptus urophydis* (*Eucalyptus urophylla* × *Eucalyptus camaldulensis*) were collected from Yangjiang Forest Farm, Guangdong Province, P.R. China. Eighteen-year-old *Eucalyptus camaldulensis* was collected from the Forest Farm of Central South University of Forestry and Technology, P.R. China. Sample chips were processed from fresh material and completely dried in a vacuum drying oven at 55 °C

under 0.01 MPa vacuum pressure. About 200-mesh powder was sieved out using an AS200 Sieving Instrument. Lignocellulosic biomass was obtained by benzene/ethanol, methanol and acetic ether extractions, and completely dried in vacuum drying oven at 55 °C and 0.01 MPa vacuum pressure. The benzene-ethanol solution was mixed according to a $V_{\text{benzene}}/V_{\text{ethanol}}$ ratio of 2. KOH, acetic acid, and deionized water were prepared for the subsequent experiments.

Experiment methods

Hemicelluloses separation

Five-gram samples of the above-mentioned powders of *Eucalyptus urophylla* and *Eucalyptus urophydis* lignocellulosic biomass were treated in 100 mL 17.5% KOH solution at 25 °C for 3, 6, 9, 12, 16, 20, 24 and 36 h, respectively. After treatment, the samples were filtered, then dried in air, fully dried in an oven, and finally stored in a dryer.

FTIR analysis

KBr pellets of samples were recorded on a Thermo Nicolet FT-IR spectrometer (Thermo Fisher Nicolet, 670FT-IR). Samples weighing 0.1–0.3 mg were mixed with 10–30 mg KBr. The KBr pellets were prepared for measurement. Thirty-two scans were collected per sample at a spectral resolution of 4 cm⁻¹, and the collected spectra were normalized against air. The spectral range was from 4000 to 500 cm⁻¹.

XRD analysis

After sample preparation, the samples were measured by an XD-2 diffractometer (General Analysis of Beijing General Instrument Co., Ltd., Beijing, P.R. China). The X-ray tube was Cu tube, the pipe potential was 36 kV, and the pipe current was 20 mA. The measurement method used 2θ/θ continuous scanning. A graphite crystal monochromator was used, with slit device DS = 1°, SS = 1°, RS = 0.3 mm. The rotary half-cone angle 2θ was from 5 to 42°, the scanning velocity was 2°/min; the scan step angle was 0.01. Cellulose crystallinity was calculated according to Equation (1):

$$\text{CrI} = (I_{002} - I_{\text{am}}) / I_{002} \times 100\% \quad (1)$$

where CrI is the relative percentage crystallinity; I_{002} is the intensity of the peak at 002 of the crystal region; I_{am} is the diffracted intensity of the peak at 2θ=18° in the amorphous region.

UV analysis

The lignin content in the wood was determined by the acetyl bromide method as follows: 10–25 mg of degreased wood powder was weighed accurately, then placed in test tubes with 10 ml of 25% acetyl bromide in acetic acid solution. The test tubes were kept in a water bath for 30 min at 70 °C without shaking for the first 15 min, then shaken every 3–5 min for 15 min to dissolve the wood powder. The tubes were cooled,

then the material transferred from the test tubes to a 100 mL volumetric flask containing 9 mL of 2 mol/L NaOH and 50 mL acetic acid. The tubes were then flushed with a small amount of acetic acid solution to make sure the transfer was complete and 1 mL of 7.5 mol/L hydroxylamine hydrochloride ($\text{NH}_2\text{OH}\cdot\text{HCL}$) was added into the flask. Finally, acetic acid was used to bring the volume to 100 mL. The absorbance of the solution at 280 nm was determined and the lignin content of the samples was calculated according to Eq. (2): $\text{Lignin content} = 100(A_s - A_b) \cdot V / \text{amd} - B(\%)$ (2) where A_s is the absorbance of the sample; A_b is the absorbance of an empty sample; V is the volume of solution (L); A is the standard absorption coefficient of lignin ($\text{g}^{-1}\text{cm}^{-1}$); m is the sample quantity (g); B is a correction factor; and d is the thickness of the cuvettes (cm). The sample solutions were measured by a UV-Vis SP-752 Spectrophotometer (Shanghai Spectrum Instrument Co., Ltd., Shanghai, P.R. China) using the following conditions: wavelength range 190–1100 nm/200–1000 nm; optical system: single beam, auto-collimation-type optical path.

SEM observations

The sample surfaces were coated in a vacuum evaporator with a thin film of Au and observed using a JSM6490LV microscope (Japan Electron Optics Laboratory Co., Ltd).

RESULTS AND DISCUSSION

Changes in lignin during hemicelluloses separation

Lignin is one of the main components of the cell wall of wood. In this study, the content of lignin was measured by UV and the results are listed in Table 1.

The lignin contents of untreated *Eucalyptus urophydis*, *Eucalyptus urophydis*, *Eucalyptus camaldulensis* were of 19.63, 20.71 and 21.14%, respectively. The statistical results show that the lignin contents were of 16.08, 16.56, 15.61, 14.60, 17.84, 16.62, 18.11 and 15.57% when the treatment times were 3, 6, 9, 12, 16, 20, 24, and 36 h, respectively. This suggests that the lignin content of the three *Eucalyptus* lignocellulosic biomass samples was reduced as measured by UV measurement during high-concentration KOH extraction. The lignin content of *Eucalyptus urophydis* was reduced from 19.63 to 9.53%; the maximum was 17.27% (6 h) and the minimum was 9.53% (3 h). The lignin content of *Eucalyptus urophydis* was reduced from 20.71 to 12.33%; the maximum was 19.73% (36 h) and the minimum was 12.33% (12 h). The lignin content of *Eucalyptus camaldulensis* was reduced from 21.14 to 15.44%; the maximum was 19.80% (3 h)

and the minimum was 15.44% (36 h). The lignin contents of *Eucalyptus urophydis*, *Eucalyptus urophydis*, *Eucalyptus camaldulensis* were reduced by 10.1, 8.38, and 5.7%, respectively. The results indicated that the molecular structure of lignin was affected by the high-concentration KOH solution, and that the lignin content changes revealed the occurrence of a dynamic process during KOH extraction.

Crystallinity changes during hemicelluloses separation

CrI was calculated by XRD, and O'KI and NO'KI index was calculated based on the FTIR spectra. The band at 1430 cm^{-1} was assigned to CH_2 shear vibration; the band at 893 cm^{-1} was assigned to glycosidic vibration and the vibration deformation of the first carbon atom; the band at 1372 cm^{-1} was assigned to C-H vibration deformation; the band at 2900 cm^{-1} was assigned to C-H and CH_2 stretching vibration. The ratios of band-heights at 1430 and 893 cm^{-1} ($\text{O'KI} = A_{1429}/A_{893}$) and at 1372 and 2900 cm^{-1} ($\text{NO'KI} = A_{1372}/A_{2900}$) have been used as relative measures of cellulose crystallinity. The results are listed in Table 2.

As shown in Table 2, the crystallinity of *Eucalyptus urophydis* lignocellulosic biomass first increased, then decreased when the treatment time was prolonged, and reached a maximum of 63.49% at 6 h. This result suggested that part of hemicelluloses in the cell wall were removed after 6 h. O'KI and CrI changed similarly, but NO'KI changed inversely.

The crystallinity index (CrI) of *Eucalyptus urophydis* lignocellulosic biomass first increased, then decreased when the treatment time was prolonged, and reached a maximum of 58.29% at 3 h. This result implied that hemicelluloses in cellulose in the amorphous region were separated after 3 h. O'KI and CrI changed similarly, but NO'KI changed inversely.

The CrI of *Eucalyptus camaldulensis* lignocellulosic biomass first increased, then CrI decreased as the treatment time was prolonged, and the value reached a maximum of 60.70% at 9 h. This result suggested that the amorphous hemicelluloses were separated after 9 h. O'KI and CrI changed similarly, but NO'KI changed inversely. However, as the pretreatment time further increased, the CrI of the pretreated biomass was sharply reduced. The potential reason for this could be attributed to the alkaline swelling action of KOH during pretreatment.

Table 1
Lignin content during hemicelluloses separation from *Eucalyptus* lignocellulose (%)

| Treatment time [h] | <i>Eucalyptus urophydis</i> | <i>Eucalyptus urophyinis</i> | <i>Eucalyptus camaldulensis</i> |
|--------------------|-----------------------------|------------------------------|---------------------------------|
| 0 | 19.63 | 20.71 | 21.14 |
| 3 | 9.53 | 18.91 | 19.80 |
| 6 | 17.27 | 14.86 | 17.55 |
| 9 | 15.61 | 14.86 | 16.36 |
| 12 | 13.60 | 12.33 | 17.87 |
| 16 | 16.94 | 17.98 | 18.59 |
| 20 | 16.04 | 18.28 | 15.54 |
| 24 | 17.02 | 19.23 | 18.07 |
| 36 | 11.54 | 19.73 | 15.44 |

Table 2
Crystallinity of *Eucalyptus* lignocellulosic biomass treated with KOH solution

| Time [h] | <i>Eucalyptus urophydis</i> | | | <i>Eucalyptus urophyinis</i> | | | <i>Eucalyptus camaldulensis</i> | | |
|----------|-----------------------------|------|-------|------------------------------|------|-------|---------------------------------|------|-------|
| | CrI [%] | O'KI | NO'KI | CrI [%] | O'KI | NO'KI | CrI [%] | O'KI | NO'KI |
| 0 | 55.10 | 1.93 | 1.53 | 56.58 | 2.18 | 1.41 | 48.31 | 1.90 | 1.61 |
| 3 | 56.22 | 2.21 | 1.37 | 58.29 | 1.96 | 1.36 | 55.45 | 2.06 | 1.32 |
| 6 | 63.49 | 2.63 | 1.43 | 56.59 | 1.90 | 1.36 | 57.05 | 2.03 | 1.37 |
| 9 | 48.77 | 2.45 | 1.49 | 52.15 | 1.87 | 1.31 | 60.7 | 2.67 | 1.58 |
| 12 | 57.36 | 2.59 | 1.52 | 51.74 | 3.27 | 1.67 | 50.36 | 2.72 | 1.51 |
| 16 | 57.73 | 2.14 | 1.37 | 54.2 | 3.10 | 1.30 | 53.26 | 2.29 | 1.46 |
| 20 | 47.62 | 3.67 | 1.04 | 54.3 | 2.10 | 1.41 | 44.42 | 2.83 | 1.36 |
| 24 | 55.38 | 1.93 | 1.30 | 52.32 | 2.00 | 1.38 | 44.39 | 2.39 | 1.33 |
| 36 | 56.21 | 3.32 | 1.68 | 46.00 | 4.61 | 1.66 | 22.90 | 4.34 | 1.70 |

Bond breaking characteristics during hemicelluloses separation

The FTIR spectra of samples of *Eucalyptus urophydis*, *Eucalyptus urophyinis* and *Eucalyptus camaldulensis* lignocellulosic biomass during hemicelluloses separation are shown in Figures 1, 2 and 3, respectively.

The bands in FT-IR spectra (Figure 1) were assigned as follows. The signals observed at 3417 cm^{-1} were related to -OH stretching vibrations (not shown in the current spectra). The peaks at 1720–1740 cm^{-1} , 1460, 1370, 1235, 1205, 1160, 1050, and 1030 cm^{-1} were assigned to the C=O stretching vibration of acetyl xylan, C-H bending vibration of chitosan, CO-OR stretching vibration of acetyl xylan, O-H in-plane bending vibration of hemicelluloses, C-O-C stretching vibration of hemicelluloses, C-O stretching vibration of acetyl xylan, and the C-O stretching vibration of

hemicelluloses, respectively. The absorbance of peaks at 3417 cm^{-1} increased from 0.959 to 1.000 at 12 h. The absorbance of peaks at 1720–1740 cm^{-1} reduced from 0.321 to 0.066 at 24 h, the absorbance of peaks at 1460 cm^{-1} increased from 0.445 to 0.806 at 36 h, the absorbance of peaks at 1370 cm^{-1} increased from 0.489 to 0.862 at 36 h, the absorbance of peaks at 1235 cm^{-1} reduced from 0.579 to 0.381 at 20 h, the absorbance of peaks at 1205 cm^{-1} reduced from 0.402 to 0.292 at 20 h, the absorbance of peaks at 1160 cm^{-1} increased from 0.663 to 0.565 at 20 h, the absorbance of peaks at 1050 cm^{-1} reduced from 1.000 to 0.789 at 20 h, and the absorbance of peaks at 1030 cm^{-1} reduced from 0.954 to 0.760 at 20 h. After the treatment in KOH solution, the C=O peak disappeared and the peaks for CO-OR, O-H and C-O abated, indicating that the acetyl groups in hemicelluloses were mostly cleaved as a result of alkali hydrolysis.

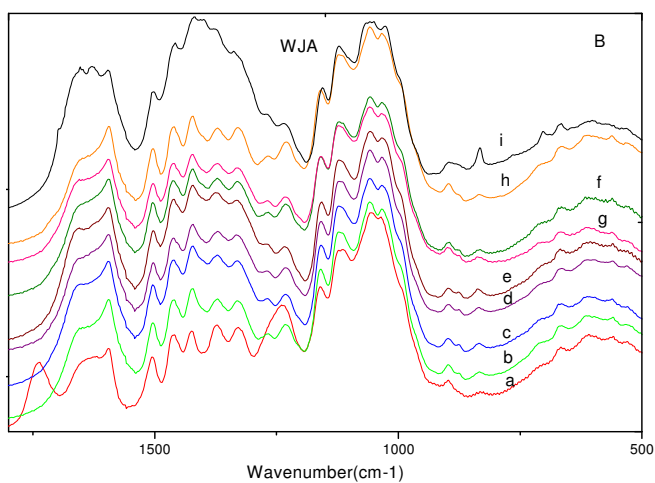


Figure 1: FTIR spectra of samples of *Eucalyptus urophydis* lignocellulosic biomass after hemicelluloses separation; (a) 0 h, (b) 3 h, (c) 6 h, (d) 9 h, (e) 12 h, (f) 16 h, (g) 20 h (h) 24 h, (i) 36 h

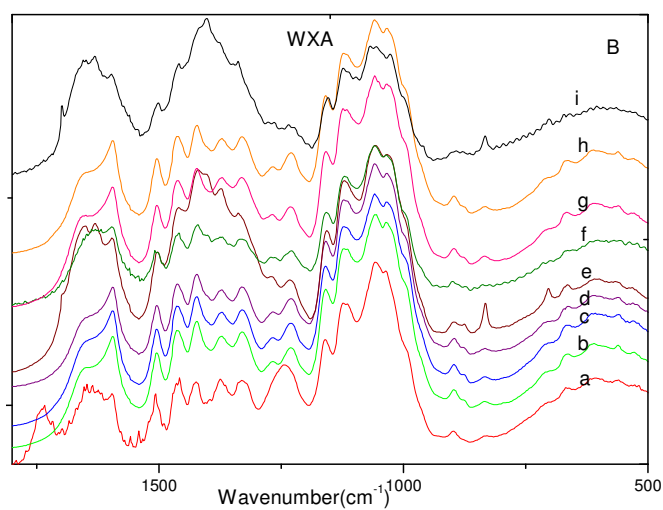


Figure 2: FTIR spectra of samples of *Eucalyptus urophydis* lignocellulosic biomass after hemicelluloses separation; (a) 0 h, (b) 3 h, (c) 6 h, (d) 9 h, (e) 12 h, (f) 16 h, (g) 20 h, (h) 24 h, (i) 36 h

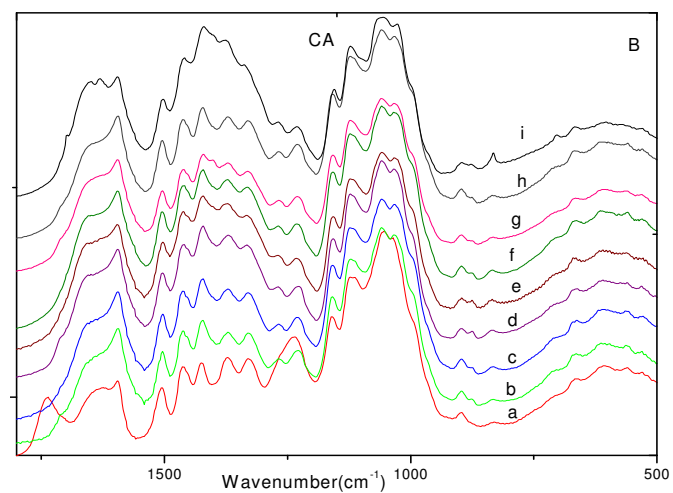


Figure 3: FTIR spectra of samples of *Eucalyptus camaldulensis* lignocellulosic biomass during hemicelluloses separation; (a) 0 h, (b) 3 h, (c) 6 h, (d) 9 h, (e) 12 h, (f) 16 h, (g) 20 h, (h) 24 h, (i) 36 h

The spectra in Figure 2 were assigned as follows. The signals observed at 3417 cm^{-1} were related to -OH stretching vibrations. The peaks at $1720\text{--}1740\text{ cm}^{-1}$, 1460 , 1370 , 1235 , 1205 , 1160 , 1050 , and 1030 cm^{-1} were ascribed to the C=O stretching vibration of acetyl xylan, the C-H bending vibration of chitosan, the CO-OR stretching vibration of acetyl xylan, the O-H in-plane bending vibration of hemicelluloses, the C-O-C stretching vibration of hemicelluloses, the C-O stretching vibration of acetyl xylan, and the C-O stretching vibration of hemicelluloses, respectively. The absorbance of peaks at 3417 cm^{-1} increased to 1.000 at 36 h. The absorbance of peaks at $1720\text{--}1740\text{ cm}^{-1}$ reduced from 0.278 to 0.041 at 16 h, the absorbance of peaks at 1460 cm^{-1} increased from 0.395 to 0.738 at 12 h, the absorbance of peaks at 1370 cm^{-1} increased from 0.390 to 0.815 at 12 h, the absorbance of peaks at 1235 cm^{-1} reduced from 0.450 to 0.235 at 36 h, the absorbance of peaks at 1205 cm^{-1} reduced from 0.302 to 0.170 at 16 h, the absorbance of peaks at 1160 cm^{-1} reduced from 0.556 to 0.349 at 36 h, the absorbance of peaks at 1050 cm^{-1} increased from 0.883 to 1.000, and the absorbance of peaks at 1030 cm^{-1} reduced from 0.810 to 0.527 at 36 h. After the treatment in KOH solution, the C=O peak disappeared, and the peaks for CO-OR, O-H and C-O abated, indicating that the acetyl groups in hemicelluloses were mainly cleaved during alkaline treatment.

The spectra in Figure 3 were assigned as follows. The signals observed at 3417 cm^{-1} were related to -OH stretching vibrations. The peaks at $1720\text{--}1740\text{ cm}^{-1}$, 1460 , 1370 , 1235 , 1205 , 1160 , 1050 , and 1030 cm^{-1} were attributed to the C=O stretching vibration of acetyl xylan, the C-H bending vibration of hemicelluloses, the CO-OR stretching vibration of acetyl xylan, the O-H in-plane bending vibration of hemicelluloses, the

C-O-C stretching vibration of hemicelluloses, the C-O stretching vibration of acetyl xylan, and the C-O stretching vibration of hemicelluloses, respectively. The absorbance of peaks at 3417 cm^{-1} increased from 0.988 to 1.000 at 9 h. The absorbance of peaks at $1720\text{--}1740\text{ cm}^{-1}$ reduced from 0.288 to 0.070 at 20 h, the absorbance of peaks at 1460 cm^{-1} increased from 0.418 to 0.640 at 16 h, the absorbance of peaks at 1370 cm^{-1} increased from 0.458 to 0.681 at 36 h, the absorbance of peaks at 1235 cm^{-1} reduced from 0.546 to 0.314 at 36 h, the absorbance of peaks at 1205 cm^{-1} reduced from 0.382 to 0.215 at 36 h, the absorbance of peaks at 1160 cm^{-1} increased from 0.633 to 0.476 at 36 h, the absorbance of peaks at 1050 cm^{-1} reduced from 0.998 to 0.754 at 20 h, and the absorbance of peaks at 1030 cm^{-1} reduced from 0.936 to 0.733 at 20 h. After the treatment in KOH solution, the C=O peak disappeared, and the peaks for CO-OR, O-H and C-O abated, indicating that the acetyl groups in hemicelluloses were mainly broken down during alkaline treatments.

SEM observations during hemicelluloses separation

Hemicelluloses, which are also known as polyose, naming any of several heteropolymers, occur along with cellulose and lignin in almost all wood cell walls. Cellulose is crystalline and resistant to hydrolysis, while hemicelluloses have a random and amorphous structure. Thus, the cell wall structure would change when cellulose and lignin are damaged to a certain extent during hemicelluloses separation. The following example of *Eucalyptus urophydis* wood revealed changes in cell wall structure. Figure 4 shows an SEM image of *Eucalyptus urophydis* wood before and after extraction in the organic solvents.

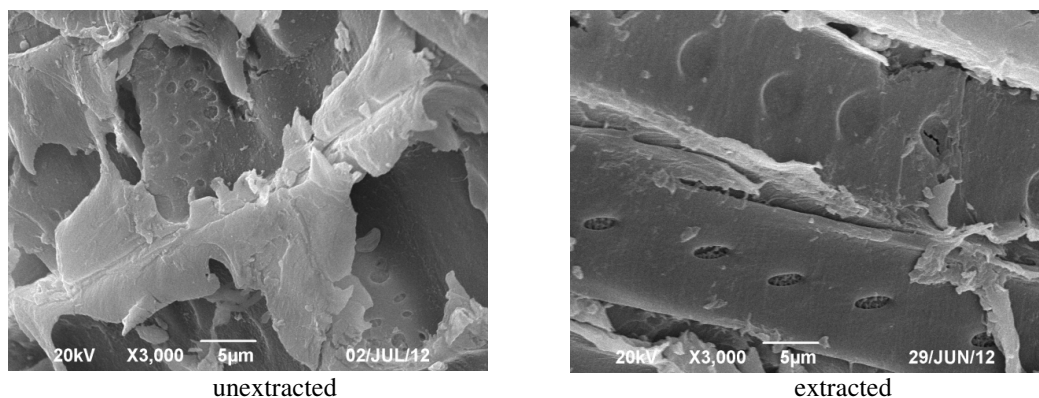


Figure 4: SEM images of *Eucalyptus urophydis* wood cell wall before and after extraction with organic solvents

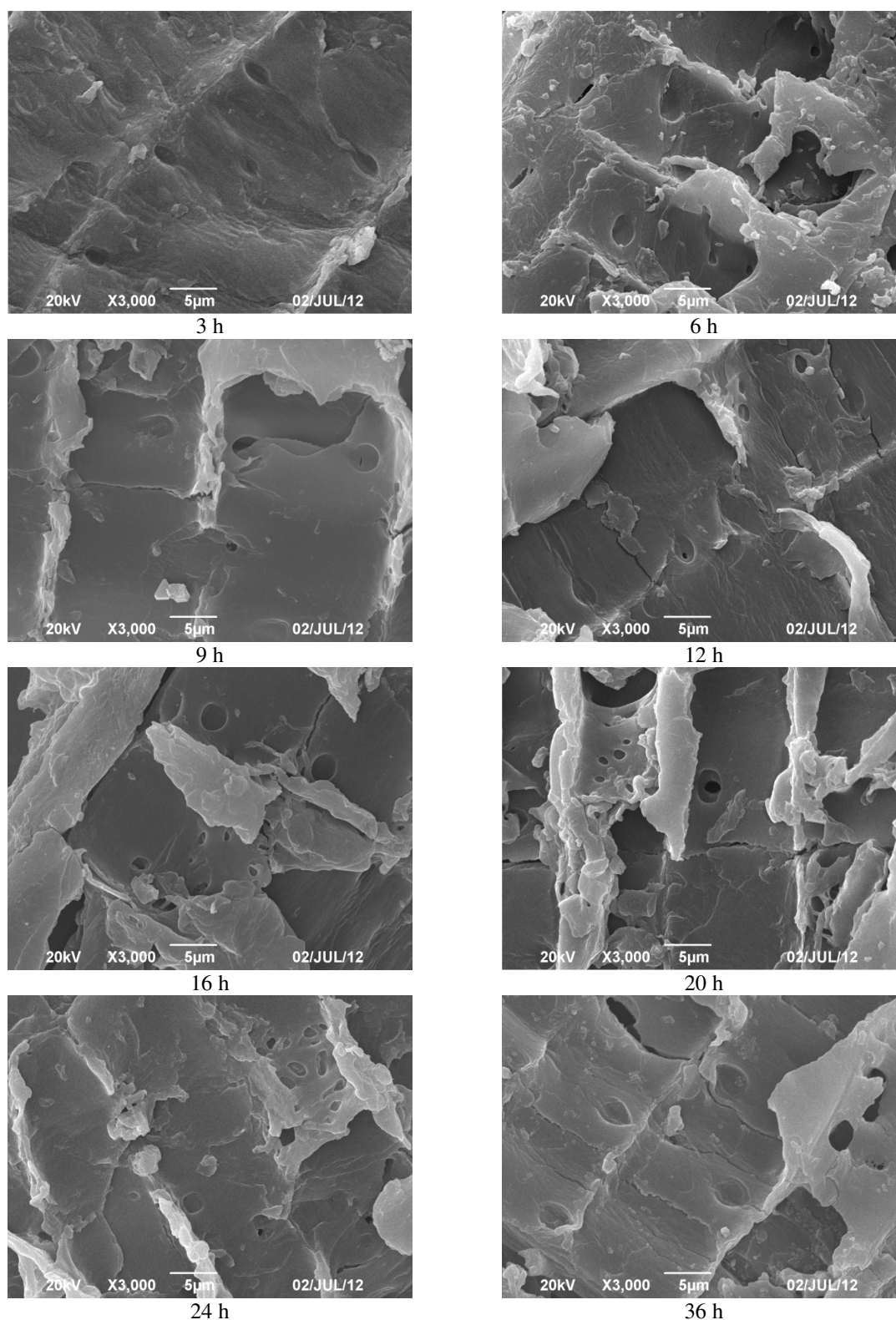


Figure 5: SEM images of *Eucalyptus* wood cell wall after separation with alkaline solution

Figure 5 shows an SEM image of *Eucalyptus urophydis* wood during hemicelluloses separation at different periods.

As shown in Figure 4, *Eucalyptus urophydis* wood was rich in extractives, which were deposited

on the surface of cell cavities, wood catheter, pit aperture, pit cavity, the gap between the microfibril of the pit membrane and other gaps, and the pits of the cell wall became fuzzy. However, the extractives were leached out, and the pits of the cell

wall became clear after wood was extracted step-by-step by benzene-alcohol, methanol, and acetic ether extraction.

The cell wall of *Eucalyptus urophydis* lignocellulosic biomass during hemicelluloses separation was observed by SEM. Figure 5 shows the change process in the cell wall of *Eucalyptus urophydis* lignocellulosic biomass during hemicelluloses separation. The microstructure was only slightly changed and hemicellulose was separated from the cell wall of *Eucalyptus urophydis* lignocellulosic biomass and dissolved into the KOH solution after 3 h. The pit membrane of the cell wall began to decompose at 6 h and was destroyed after 9 h. The cell wall gradually thinned from 9 to 20 h of hemicelluloses separation time. When hemicelluloses were separated for 20 h, the pit membrane was dissolved, pits appeared to be penetrated, there were holes in the cell wall, and cell gaps were also opened. Hemicelluloses seemed to have dissolved into the KOH solution after 36 h. However, more investigations need to be done to confirm this in future studies.

CONCLUSION

During hemicelluloses separation in KOH solution, the crystallinity of *Eucalyptus urophydis*, *Eucalyptus urophydis* and *Eucalyptus camaldulensis* lignocellulosic biomass reached maxima of 63.49% at 6 h, 58.29% at 3 h, and 60.70% at 9 h, respectively, suggesting that hemicelluloses were probably mostly removed during these periods. However, the lignin contents of *Eucalyptus urophydis*, *Eucalyptus urophydis*, *Eucalyptus camaldulensis* were reduced by 10.1, 8.38, and 5.7%, respectively. The FTIR spectra results suggested that the acetyl groups in hemicelluloses were mainly broken down during alkaline treatments. Further SEM observations also provide more visual evidence to support the separation process. However, more investigation needs to be done to address the inherent reasons for different regularities of different species.

ACKNOWLEDGMENTS: This work was financially supported by the National Natural Science Foundation of China (No. 31070497), the Program for New Century Excellent Talents in University (No. NCET-10-0170), the Scientific Research Fund of Hunan Provincial Education Department (No. 10A131), and was a Key Project of the Chinese Ministry of Education (No. 211128).

REFERENCES

- ¹ A. K. Chandel, G. Chandrasekhar, K. Radhika, R. Ravinder, P. Ravindra, *Biotechnol. Mol. Biol. Rev.*, **6**, 8 (2011).
- ² B. C. Saha, *J. Ind. Microbiol. Biotechnol.*, **30**, 279 (2003).
- ³ L. Viikari, M. Tenkanen, J. Buchert, M. Ratto, M. Bailey *et al.*, in “Bioconversion of Forest and Agricultural Plant Residues”, edited by J. N. Saddler, CAB, Oxford, 1993, pp. 131-182.
- ⁴ K. K. Y. Wong, L. U. L. Tan and J. N. Saddler, *Microbiol. Rev.*, **52**, 305 (1988).
- ⁵ J. G. Zeikus, E. Lee, Y. E. Lee, B. C. Saha, in “Enzymes in Biomass Conversion”, edited by G. F. Leatham and M. E. Himmel, American Chemical Society, Washington, D.C., 1991, pp. 36-51.
- ⁶ H. V. Scheller and P. Ulvskov, *Ann. Rev. Plant. Biol.*, **61**, 263 (2010).
- ⁷ G. Hoch, *Func. Ecol.*, **21**, 823 (2007).
- ⁸ B. C. Saha, *J. Ind. Microbiol. Biotechnol.*, **30**, 279 (2003).
- ⁹ N. Moiser, C. Wyman, B. Dale, R. Elander, Y. Y. Lee *et al.*, *Bioresour. Technol.*, **96**, 673 (2005).
- ¹⁰ A. K. Chandel, O. V. Singh and L. V. Rao, in “Sustainable Biotechnology: Renewable Resources and New Perspectives”, edited by O. V. Singh and S. P. Harvey, Springer Verlag, 2010, pp. 63-81.
- ¹¹ M. M. Wu, D. J. Gregg, A. Boussaid, R. P. Beatson, J. N. Saddler *et al.*, *Appl. Biochem. Biotech.*, **77**, 47 (1999).
- ¹² G. Brodeur, E. Yau, K. Badal, J. Collier, K. B. Ramachandran *et al.*, *Enzyme Res.*, **1**, 1 (2011).
- ¹³ J. L. Wen, Y. C. Sun, F. Xu, R. C. Sun, *J. Agric. Food Chem.*, **58**, 11372 (2010).
- ¹⁴ T. Song, A. Pranovich, H. Bjarne, *Holzforchung*, **65**, 35 (2011).
- ¹⁵ T. Song, A. Pranovich and B. Holmbom, *Bioresour. Technol.*, **102**, 10518 (2011).
- ¹⁶ E. J. Mellerowicz and B. Sundberg, *Curr. Opin. Plant. Biol.*, **11**, 293 (2008).
- ¹⁷ F. Peng, J. L. Ren, F. Xu, J. Bian, P. Peng *et al.*, *J. Agric. Food Chem.*, **57**, 6305 (2009).
- ¹⁸ M. Subba Rao and G. Muralikrishna, *J. Agric. Food Chem.*, **54**, 2342 (2006).
- ¹⁹ M. R. Cyran and L. Saulnier, *J. Agric. Food Chem.*, **55**, 2329 (2007).
- ²⁰ T. Pepper and P. M. Olinger, *Food Technol.*, **42**, 98 (1988).
- ²¹ E. Winkelhausen and S. Kuzmanova, *J. Ferment. Bioeng.*, **86**, 1 (1998).
- ²² W. B. Wei, L. N. Li, L. Chang, Z. Wang, *J. Appl. Polym. Sci.*, **130**, 2390 (2013).
- ²³ T. A. Gulbrandsen, I. A. Johnsen, M. T. Opedal, K. Toven, K. Øyaas *et al.*, *Cellulose Chem. Technol.*, **49**, 117 (2015).
- ²⁴ H. Ren, S. Omori, *Cellulose Chem. Technol.*, **48**, 675 (2014).